

THE PATTERN OF CELL SURVIVAL IN THE PIG LIVER FOLLOWING ONE FREEZE-THAW CRYOSURGERY CYCLE

Jianfei Ye¹, Franco Lugnani^{2*}, Ling Yuan³, John GJ Zhao⁴, Diana Zhang⁴
and Boris Rubinsky⁵

¹ Department of Surgery, Tianjin Haibin People's Hospital, Tianjin, P.R. China.

² Hippocrates D.O.O, Divaca, Slovenia.

³ Tianjin Institute of Medical Science, Tianjin, P.R. China.

⁴ Medinux (Tianjin) Technologies Co., Ltd., Tianjin, P.R. China.

⁵ Department of Mechanical Engineering, University of California Berkeley, Berkeley, CA, USA.

*Corresponding author's E-mail: franco.lugnani@gmail.com

Abstract

BACKGROUND: It is well established that in cryosurgery some cells can survive one freeze thaw cycle and that surviving cells are found at the margin of the frozen lesion. Numerous techniques are being developed to ensure the survival of frozen cells to the margin of the frozen region. **OBJECTIVE:** We thought that it would be of fundamental interest to observe the pattern of cell survival in a liver treated with one freeze-thaw cycle. **MATERIALS AND METHODS:** We performed six ultrasound-guided single freeze-thaw cryosurgery procedures on the liver of four Landrace pigs, using two cryosurgery probes separated by 25 mm inserted in parallel. Treated organs were removed 24 hours after the cryosurgery and processed for histology with hematoxylin and eosin. The tissues were analyzed with a digital slice scanner. **RESULTS:** We found an unexpected pattern of cell survival; sheets of live cells, about 200 µm in width, that follow the network of interlobular connective tissue septae to a distance of several millimeter from the outer edge of the one freeze-thaw cycle cryosurgery treated lesion. The sheets of live cells surround lobule cores that have undergone complete coagulative necrosis. In addition, larger blood vessels, as far as 5 mm from the outer rim of the treated lesion, have a major and complex effect on cell survival with large areas of completely necrotic and completely alive cells intermixed. **CONCLUSION:** This study may have value as a baseline for developing new cryosurgery protocols designed to ablate cells to the margin of the frozen lesion.

Keywords: cryosurgery; interlobular connective tissue septae; large blood vessels; tissue ablation.

INTRODUCTION

In cryosurgery undesirable tissues are frozen in the hope that they will be ablated by freezing (1, 2, 3, 4). Liver is an important target for tissue ablation by cryosurgery (5). Freezing is induced by a cryosurgery probe, cooled internally with a cryogen, inserted in the core of the tumor. The frozen lesion propagates in time from the cryosurgery probe outward. Cryosurgery has

many attractive clinical attributes, including the ability to monitor the extent of the frozen lesion in real time with medical imaging (6, 7, 8, 9, 10). While medical imaging monitors the extent of the frozen lesion, fundamental research shows that cells can survive freezing under conditions that exist at the margin of the frozen lesion (11, 12, 13). Animal studies provide evidence that indeed, cells survive freezing on the outer rim of a cryo-lesion (14). It is obvious that a cryosurgery

technology that ablates to the margin of the frozen region would have clinical value, when used in combination with medical imaging. Extensive and imaginative research is being conducted on technologies to ablate cells to the margin of frozen lesions (15, 16, 17, 18).

While numerous previous studies report cell survival at the margin of the frozen lesion (e.g., 14), the exact pattern of survival is not described. It would be of fundamental interest to observe the pattern of cell survival in a liver treated with a one freeze-thaw cycle. The present work aimed to generate such information. Taking the advantage of digitized histology analysis (K-Viewer, Ningbo KFBIO, China), we have examined the histology of hematoxylin and eosin (H&E) stained pig liver, frozen with a one freeze-thaw cycle, 24 hours after the procedure. We observed an unexpected pattern of cell survival. Our original naïve expectation was that on the outer rim of the frozen lesion there is a random mix of live and dead cells, with cell survival increasing towards the margin of the frozen lesion. We find that the unexpected pattern is related to the anatomy of the liver and is different from our original naïve expectations.

MATERIALS AND METHODS

Animal model

All applicable international, national, and/or institutional guidelines for the care and use of animals were followed. After a 24 hour fast, each animal was pre-medicated with a combination of xylazine hydrochloride (600 mg) and Midazolam (20 mg) via intramuscular injection. Anesthesia with intravenously administered Propofol (350-450 mg/h) was adjusted to the heart rate. A first dose of 50 µg fentanyl was used for pain relief and 30 µg/h for maintenance. The access to the upper abdomen was obtained using a Chevron-like subcostal incision extended to the left side. Liver was then exposed and mobilized cutting the falciform ligaments. Each cryo-placement was recorded using conventional photo/video cameras and ultrasound imaging (Model IP-1223DV, Hitachi-Aloka). Six two pair probe cryosurgery lesions were performed in separate lobes of four pigs' liver. The animals were kept alive for 24 hours, under continuous monitoring with the pain prevention protocol described above.

Cryosurgery generator

An argon gas based cryosurgical device and probes was used to carry out the experiments (CryoE Knife, model CRYOE-80, Medinux). The device consists of a controlled computerized console that can deliver a constant flow of Argon gas at 3000 psi to custom-made 2.4 mm diameter dedicated sterile cryosurgery probes (CE24, Medinux) where a typical Joule Thomson expansion system liquifies the gas to generate the needed cryogenic temperature (-185.8 °C). The type of ice balls that they produce is shown in Figure 1A.

Experimental protocol

The ablative cryosurgery treatment was applied using the following protocol. First, two cryoprobes were inserted in parallel to an equal depth of 15 mm inside the liver through a custom-made Plexiglas holder with two cryoprobe compatible drilled holes separated by 25 mm. The 3000 psi argon gas was delivered simultaneously to the two parallel cryosurgery probes for 13 min. This duration of freezing and gas pressure ensured the formation of two large merging ice-balls clearly visible on the surface of the liver, as illustrated by Figure 1B. The cryoprobes were removed after 8 min of passive thawing.

Measurements

Experiments were monitored and recorded using ultrasound, video and photography. The internal control circuit of the prototype was used for temperature monitoring. A typical temperature measurement is shown in Figure 1C. The panel shows the cryosurgery probe and the arrow points to the thermocouple's location, 1 cm from the tip.

Histological examination

After liver cryosurgery, the pigs were kept alive for 24 hours and euthanized with an overdose of 200 mg propofol, and 5 min later potassium chloride. The abdomen was opened, the vena cava closed and cut to produce total bleeding. The liver was removed, placed on a table and each lesion was flushed with saline, identified, and the outer dimensions measured (Figure 1D). The lesions were bread loafed along the cryoprobes central path (Figure 1D) and soaked in 4 % PFA (RNase free) for 72 hours and then embedded in paraffine blocks. For microscopic analysis, 3 µm sections were cut from the samples and stained with H&E (Figure 1E, 1F). Micrographs were taken and digitized by

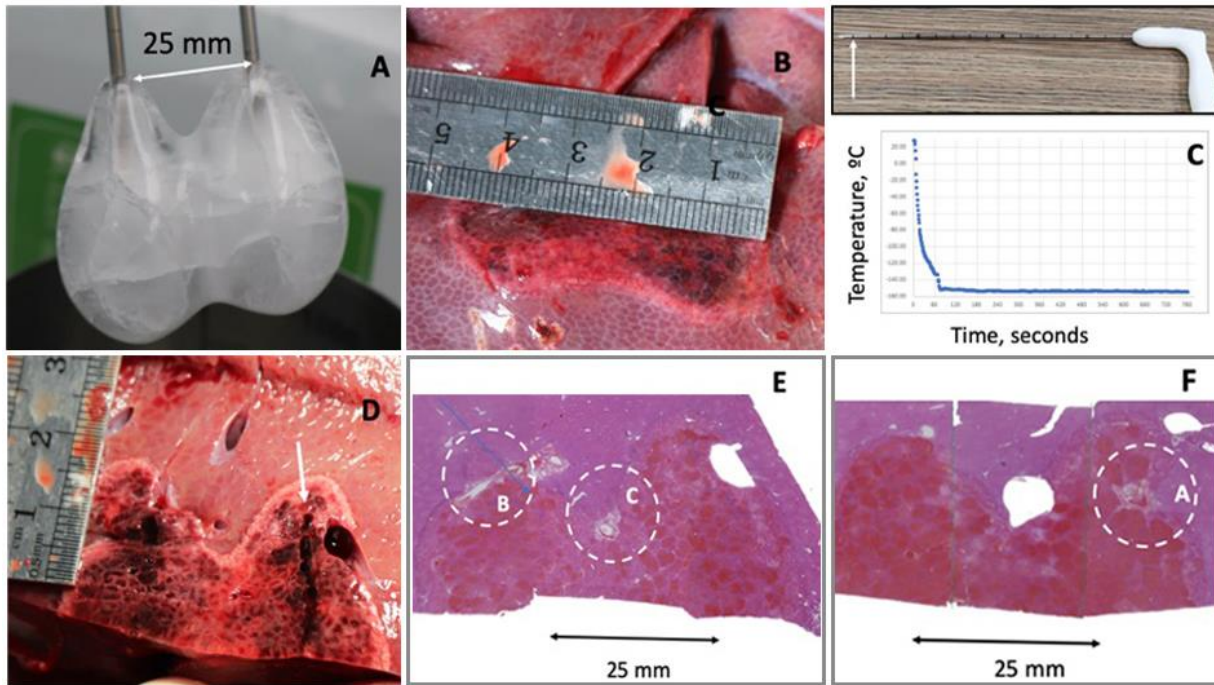


Figure 1. The experimental procedure. **A**, An image of two ice balls formed around a pair of cryosurgery probes in water using the study's freezing protocol. **B**, The appearance of the outer surface of the treated liver after a single freeze-thaw procedure. **C**, A cryosurgical probe and the temperature in time measured at the location indicated by an arrow. **D**, The cross section of a treated liver cut along the cryoprobes plane. The arrow points to the path of the cryoprobe. **E**, The H&E micrograph of panel D. **F**, Another H&E stained micrograph from another liver. The areas encircled by white dashed circles are examined with higher magnification in subsequent figures.

a digital slice scanner (Model KF-PRO-005, KFBIO Co., Ltd.).

RESULTS

Figure 1A shows two ice balls developed from a simulation of the *in vivo* cryosurgical procedure of this study in 24 °C water. The outer margin of the ice in Figure 1A is smooth and continuous and symmetric along the center plane between the cryosurgery probes, as expected from freezing in a homogeneous medium. The maximal width and height of the frozen lesion are 53.6 mm and 47 mm, respectively.

For histology, the tissue was cut along the path of cryosurgical probes on the plane of two probes. An arrow in Figure 1D points to a cryosurgery probe path. Figure 1E and 1F are macroscopic H&E slides from two experiments.

Figure 2A is a control showing normal liver hepatocytes with large and round nuclei with clear nuclear membranes. Some hepatocytes have binucleated nuclei and eosinophilic cytoplasm. Hepatic sinusoids are located between hepatic cords, and the sinus cavity is irregular. Figure 2B illustrates the typical appearance of hepatocytes

in the core of the frozen lesion. Cells in this region have experienced coagulative necrosis and pyknotic nuclei are predominant. The evidence of karyorrhexis, the destructive fragmentation of the nucleus of a dying cell which follows pyknosis, is also seen. Some nuclei have karyolysis, which is the complete degradation of the chromatin of a dying cell. The whole cells will eventually stain uniformly with eosin after karyolysis. The appearance of karyolysis after karyorrhexis occurs mainly as a result of necrosis. Figure 2C shows an unexpected feature, observed in all the experiments on the margin of the ablation lesion along the interlobular connective tissue septae. It shows the intrusion of a sheet of live cells from the outer surface of the lesion (dashed arrow) to a depth of about 0.5 mm (straight arrow). The live cells (transparent nuclei) in the intrusion are surrounded by regions of death cells, (dark pyknotic nuclei). The sheets of living cells surrounded by necrotic cells, corresponding with the interlobular connective tissue septae, can take various configurations and can be found at mm scale distances from the outer surface of the lesion. Figure 2D shows a 200 μ m sheet of mainly living cells, parallel to the outer margin of the

lesion between two layers of completely necrotic cells. Figure 2E, shows the appearance of the outer margin of the lesion. Living cells (transparent nuclei) are found between regions of dead cells (pyknotic nuclei). Scale bar 100 μm . Figure 2F, illustrates the effect of larger blood vessels on the pattern of cell survival. This is the area marked with a dashed circle and the letter A, in Figure 1F. It shows that the outer edge of the treatment lesion has an indentation of several millimeter relative to the homogeneous tissue.

Additional patterns of cell ablation are shown in Figure 3 and Figure 4. Figure 3A shows a higher magnification of the site marked with a dashed circle B, in Figure 1 E. A large vein and the adjacent artery have caused an indentation of about 4 mm in the ablation margin relative to a hypothetical ablation margin in a homogeneous tissue, (dashed line). Figure 3B shows the appearance of the cryosurgery treated tissue at the

margin of the vein. It is evident that near the vein at about 3 mm from the outer surface there is a layer of live cells. Figure 3C shows a typical interface between the layer of live cells near the vein and the region of necrotic tissue that follows, towards the exterior of the treated region. Further away, toward the outer surface of the treated lesion, are region of predominantly coagulative necrosis. However, throughout the region of coagulative necrosis there are regions of live cells (transparent nucleus) which penetrate into a region of necrotic cells (pyknotic nucleus, nuclear fragmentation and nuclear dissolution). Figure 3D is another site in the core of the treated tissue, where regions with predominantly live cells are found surrounded by large region of cells that have undergone coagulative necrosis as a rule, the region of live cells is found along the interlobular connective tissue septae. Figure 3F

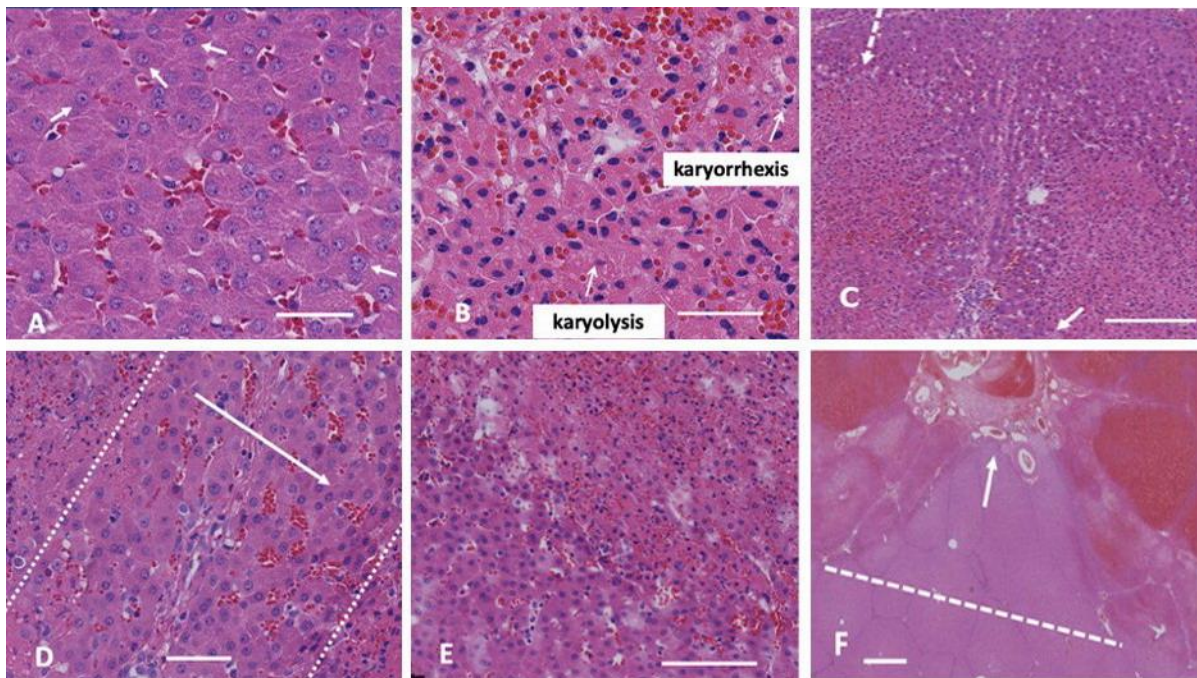


Figure 2. Various typical patterns of cell ablation. **A**, Normal liver with intact nuclei, scale bar 50 μm . **B**, Necrotic liver with pyknotic nuclei, scale bar 50 μm . **C**, A typical appearance of live cells between a region of ablated cells characterized by pyknotic (dark nuclei). Live cells are along the interlobular connective tissue septae on both sides. The dashed arrow points to the outer edge of the ablation lesion and the solid arrow point to the depth of penetration of the sheet of live cells into the ablated region, about 0.5 mm. Scale bar 200 μm . **D**, A larger magnification of living cells along the interlobular connective tissue septae, between layers of necrotic cells with a pyknotic nuclei. This image is from a section that was parallel to the outer edge of the ablated region, at mm depth from the outer surface. Arrow points to the outer edge. Scale bar 50 μm . **E**, The outer edge of the ablation lesion showing a mixture of live with necrotic cells with pyknotic nuclei, Scale bar 100 μm . **F**, A higher magnification of the area marked with a circle in Figure 1F, illustrating the effect of the portal areas which includes three accompanying ducts (interlobular vein, interlobular artery and interlobular bile duct) on the outer ablation margin. White arrow shows that the ablation has receded by over 4 mm from an edge expected in tissue without a blood vessel (dashed line). Scale bar 1 mm.

shows a micrograph from the outer margin of the treatment lesion. A group of dead cells (marked with a white line dashed oval) is surrounded by living cells. In all panels, the appearance of the necrotic tissue is comparable to the appearance of the necrotic tissue in the core of the frozen region with nuclear pyknosis, nuclear fragmentation, and nuclear dissolution in the necrotic area.

The panels in Figure 4 are a higher magnification of the area marked with a C in Figure 1E. It shows the effect of a vessel group (a large vein, two arteries and two bile ducts) on the survival of liver tissue frozen with one freeze-thaw cryosurgery cycle. We were surprised to find in the higher magnification Figure 4B that at the margin of the treated lesion the interior of the lobule is necrotic with pyknotic nuclei, while cells all around the necrotic core of the lobule are alive. Details on the way the necrotic and live

cells mix are shown in the higher magnification Figure 4C-4F. They show that cells survive around the blood vessels complex and along the interlobular connective tissue septae around the necrotic lobule core.

DISCUSSION

Attempts are being made to develop technologies or find chemical additives that would ensure cell death to the margin of the frozen lesion, with one freeze thaw cycle. In order to establish a base line for future research in such technologies, we document the effect of one single clinical freeze thaw cycle on the pig liver. In all our experiments we find that all the cells in the core of the treated volume have experienced coagulative necrosis (Figure 2B). This supports

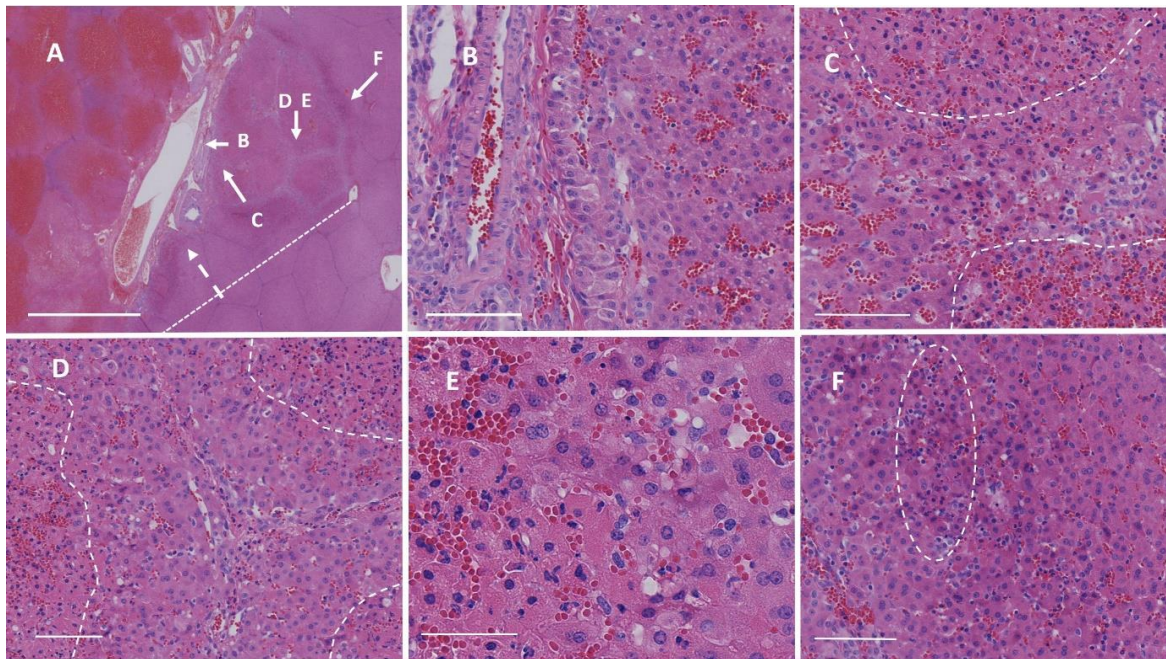


Figure 3. Combinations of different cell ablation patterns. **A**, A higher magnification of the site marked with a dashed circle B in Figure 1E. A dashed arrow points an artery and a vein. The dashed line is the hypothetical location of the ablation margin when a homogeneous medium is frozen. Arrows point to different locations in the tissue, between the vein and the outer surface of the treated region. The arrows are marked with letters corresponding to the higher magnification panels (**B**, **C**, **D**, **E**, **F**). Scale bar 2.5 mm. **B**, A layer of live cells at the margin of the vein and the appearance of tissue at the margin of the vein (bar 100 μ m). **C**, A typical interface between the layer of live cells near the vein and the region of necrotic tissue that follows (bar 100 μ m). Dotted lines separate between the regions of necrotic tissue and the regions of mixed live and dead cells. **D**, Another site in the core of the treated region, with regions with predominantly live cells surrounded by large region of cells that have undergone coagulative necrosis (bar 100 μ m). The dashed white lines separate between the regions of dead cells and regions of predominantly live cells. **E**, A higher magnification from the left-hand margin between life and dead cells in Figure 3D to show the complex pattern of life and dead cells within the treated region (bar 50 μ m), **F**, A micrograph from the outer margin of the treatment lesion showing a group of dead cells (marked with a white line dashed oval) surrounded by living cells (bar 100 μ m).

the common practice in many cryosurgery protocols in which the second freeze thaw cycle is applied only to the outer margin of the frozen lesion.

The vasculature in the liver is characterized by six portal areas around each liver lobule. The portal areas include three accompanying ducts (interlobular vein, artery and bile ducts). The interlobular connective tissue septae connect between the portal areas and separate between adjacent lobules. The thermal effect of large blood vessels on cell survival is expected. Large blood vessels can cause an indentation in the ablation margin by as much as 4 to 5 mm (Figure 2F and 3A). However, Figures 2F, 3A and 4A show that the degree and manner in which cells survive around blood vessels vary, from no dead cells in the blood vessel's proximal area (Figure 2F) to a mixture of live and dead cells all around the blood vessel in Figure 3A and Figure 4A.

Most surprising was the survival of cells in the form of sheets of live cells surrounded by

necrotic cells, to a depth of several mm from the outer surface of the lesion. We have followed the sheets of surviving cells throughout the treated livers and we find that the cells survive all along the interlobular connective tissue on both sides of the interlobular connective tissue. Hepatic lobules, the structural unit of the liver, are invaginated by a network of branched connective tissue septae. Afferent blood vessels and lymphatics follow this connective tissue structure throughout the liver. The blood vessels in the connective tissue could elevate the local temperature to avoid freezing and thereby facilitate cell survival. The surprising element is that despite the small, micron scale dimension of the interlobular connective tissue the width of the sheets of surviving cells is on the order of magnitude of 100 μm to 200 μm , and they can penetrate to a depth of several mm. Of relevance to clinical applications, the 3-4 mm region on the outer edge of the frozen lesion would have appeared completely frozen on intraoperative

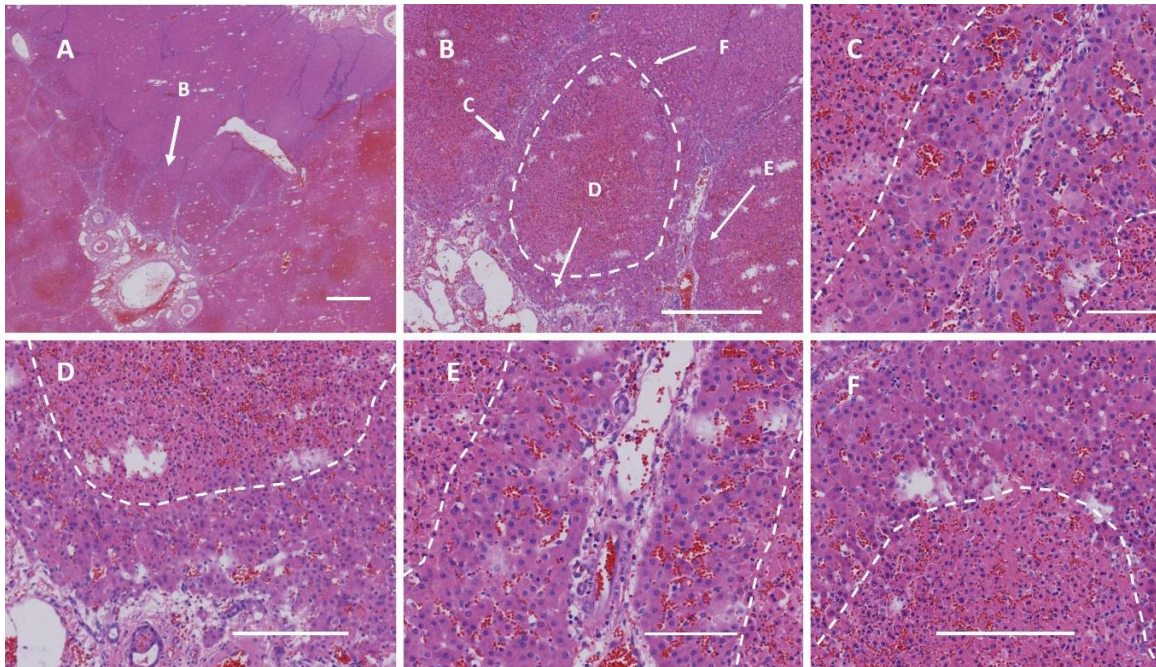


Figure 4 Combinations of different patterns of cell ablation. **A**, A higher magnification of the area marked with a C in Panel 1E. Dashed arrow points to a portal area which includes a large vein, two arteries and two bile ducts. Letter B marked arrow in Panel 4A points to the area shown at higher magnification in Panel 4B. Scale bar 1 mm. **B**, Higher magnification of the location marked with the letter B in Panel 4A. The letters which mark the arrows in panel 4B, correspond to the designation of the subsequent panels. Panel 4B illustrates a pattern observed in all the lobules on the margin of the ablated tissue in this experiment. The interior of the lobule is necrotic with pyknotic nuclei (necrotic area surrounded by a closed white dashed line), while the cells all around the necrotic core of the lobule are alive. Scale bar 0.5 mm. Details on the mixed pattern of live and dead cell are found in Figs **4C** (scale bar 100 μm), **4D** (scale bar 200 μm), **4E** (scale bar 100 μm) and **4F** (scale bar 200 μm). The dotted lines separate between the region of live cells and regions of dead cells.

imaging, when in fact it is riddled with live cells. These results should be viewed with caution as the human liver has fewer lobules than the pig liver and malignant tumors are not hepatocytes. However, many malignant tumors are highly vascularized and especially on the outer edge, and it is quite likely that this highly vascularized edge could have a similar effect on cell survival as the interlobular connective tissue septae.

This study has investigated the pattern of cell survival in the pig liver after one single freeze thaw cycle as a baseline for future research into different technologies designed to ensure complete cell ablation in the frozen lesion. After one freeze thaw cycle there can be large regions of mostly surviving cells surrounding or surrounded by large regions of complete necrosis to a depth of 3 mm to 4 mm from the outer edge of the ablation zone. The pattern of cell survival along the interconnective tissue is of particular concern, because it indicates that even small blood vessels can result in cells surviving cryosurgery protocols that employ one freeze thaw cycle.

Acknowledgements: The work was supported by National Hi-tech Enterprise Fund of China. Award Number: GR201812001835 to Medinix (Tianjin) Technologies Co., Ltd.

REFERENCES

1. Baust JG & Gage AA (2005) *Bju Int* **95**, 1187–1191.
2. Baust JG, Gage AA & Baust JM (2016) in *Dermatological Cryosurgery and Cryotherapy*, (eds) Abramovitz W, Graham G, Har-Shai Y & Strumia R, Springer, pp 9–16.
3. Gage AA (1995) in *Cryosurgery - Mechanisms and Applications*, (ed) Lucas L, Appl. Int. Inst. Refrigeration, Paris, 140 pp.
4. Gage AA, Baust JM & Baust JG (2009) *Cryobiology* **59**, 229–243.
5. Dutta P & Gage AA (1977) *Cryobiology* **14**, 687.
6. Gilbert JC, Onik GM, Hoddick WK & Rubinsky B (1984) *IEEE/Engineering Med. Biol Soc Annu Conf*, 107–111.
7. Isoda H (1989) *Nippon Igaku Hoshasen Gakkai Zasshi. Nippon Acta Radiol* **49**, 1499–1508.
8. Onik G, Cooper C, Goldberg HI, Moss AA, Rubinsky B & Christianson M (1984) *Cryobiology* **21**, 321–328.
9. Otten DM & Rubinsky B (2005) *Physiol. Meas* **26**, 503–516.
10. Rubinsky B, Gilbert JC, Onik GM, Roos MS, Wong ST & Brennan KM (1993) *Cryobiology* **30**, 191–199.
11. Baust JG, Gage AA, Bjerklund Johansen TE & Baust JM (2014) *Cryobiology* **68**, 1–11.
12. Rui J, Tatsutani KN, Dahiya R & Rubinsky B (1999) *Breast Cancer Res Treat* **53**, 185–192.
13. Tatsutani K, Rubinsky B, Onik G & Dahiya R. (1996) *Urology* **48**, 441–447.
14. Cornelis FH, Durack JC, Kimm SY, Wimmer T, Coleman JA, Solomon SB & Srimathveeravalli GA (2017) *Cardiovasc. Intervent Radiol* **40**, 1600–1608.
15. Baust JG, Gage AA, Clarke D, Baust JM & Van Buskirk R (2004) *Cryobiology* **48**, 190–204.
16. Baust JG, Bischof JC, Jiang-Hughes S, Polascik TJ, Rukstalis DB, Gage AA & Baust JM (2015) *Prostate Cancer Prostatic Dis* **18**, 87–95.
17. Pham L, Dahiya R & Rubinsky B (1999) *Cryobiology* **38**, 169–175.
18. Stewart GJ, Preketes A, Horton M, Ross WB & Morris DL (1995) *Cryobiology* **32**, 215–219.